CHEMICAL, MATHEMATICAL, PHYSICAL SCIENCES DIVISION

CMPSD-1

ON ANTI-CONVEXITY AND FORCING CONVEXITY IN GRAPHS

Lyndon B. Decasa [1] and Sergio R. Canoy, Jr. [2]

[1]Department of Mathematics
Northern Mindanao State Institute of Science and Technology, Butuan City
E-mail: lyndon_decasa2003@yahoo.com
[2]Department of Mathematics, College of Science and Mathematics
Mindanao State University - Iligan Institute of Technology, Iligan City
e-mail: csm-src@sulat.msuiit.edu.ph

This study seeks to define the anti-convexity and forcing convexity concepts in graphs and give some characterizations of graphs with a specified anti-convexity number and forcing convexity number. Furthermore, it aims to show that the anti-convexity number of a connected graph G consisting of k extreme vertices is equal to k, and determine the anti-convexity numbers of some graphs. Also, we show that the forcing convexity number of a connected graph G of order $n \geq 1$ is $n-1$ if and only if it is complete graph K_n. Moreover, we characterize those connected graphs G such that $fcon(G)=con(G)$.

The study obtained the following results:

1. If G is a connected graph with k-complete vertices, then $acon(G)=k$.
2. Let G be connected of order n. Then $acon(G)=n$ if and only if $G=K_n$.
3. Let $F_{m,n}$ be the generalized fan of order $m+n$. Then
   (a) $acon(F_{m,n})=2$ if $m=1$ and $n\geq 3$ or $m\geq 2$ and $n\geq 3$ or $m=n=1$;
   (b) $acon(F_{m,n})=m$ if $m\geq 2$ and $n\geq 1,2$;
   (c) $acon(F_{m,n})=3$ if $m=1$ and $n=2$.

4. Let $W_{m,n}$ be the generalized wheel of order $m+n$, where $m\geq 1$ and $n\geq 3$. Then
   (a) $acon(W_{m,n})=\frac{n}{2}$ if n is even;
   (b) $acon(W_{m,n})=\frac{n+1}{2}$ if n is odd;
   (c) $acon(W_{m,n})=4$ if $m=1$ and $n=3$;
   (d) $acon(W_{m,n})=m$ if $m\geq 2$ and $n=3$;
   (e) $acon(W_{m,n})=2$ if $m\geq 2$ and $n>3$.

5. Let G and H be non-complete graphs such that $acon(G+H)\neq 1$. Then $acon(G+H)=2$.
6. If G is any graph with $Ext(G)=o$, then $acon(G+H)=|Ext(G)|$.
7. Let G be a connected graph. If S is a maximum convex set in G, then S is a forcing subset for itself. In particular,
8. Let G be a connected graph. If G has a unique maximum convex set S, then the empty set ϕ is a forcing subset for S. In this case,
9. Let G be a connected graph with k-complete vertices ($k\geq 1$).
Then $fcon(G)=k-1$.
10. Let K_n be the complete graph of order $n\geq 1$. Then $fcon(K_n)=n-1$ if and only if $G=K_n$.
11. Let G be a connected graph of order $n\geq 3$. Then $fcon(G)=con(G)$ if and only if for every maximum convex set S of G, $\langle S\rangle$ is complete and $fcon(S)=|S|$.

Keywords: graph, convex, anti-convexity number, forcing convexity number, complete, join, set of extreme vertices

CMPSD-2

INDUCED CYCLE ACCESSIBILITY NUMBER OF A GRAPH

John Benedict T. Ayawan, Kimberly Hazel B. Camino*, Marve Ann A. Echavez, Meldren C. Garong, Joan B. Ybañez, and Rosalio G. Artes, Jr.

Department of Mathematics, College of Science and Mathematics
Mindanao State University - Iligan Institute of Technology
Andres Bonifacio Avenue, Tibanga, 9200 Iligan City
Email: *misyr_khbc@yahoo.com.ph

Given a connected graph G, we define the distance $d_G(u,v)$ between two vertices u and v in G as the length of a shortest path joining u and v in G. For any positive integer m greater than 2, we define an m-cycle of G as a cycle in G of order m induced by a subset of $V(G)$. We say that G is an m-cycle k-accessible graph if G contains an m-cycle C_m such that for every vertex v in the vertex set of G, there exists a vertex u in the vertex set of C_m such that the distance between vertices u and v in G is at most k. The m-cycle accessibility number of G is given by $h_m(G)=\min\{k: G \text{ is an } m\text{-cycle } k\text{-accessible graph}\}$. We use the convention that whenever a connected graph G has no cycle of order m, then we denote by positive infinity its corresponding m-cycle accessibility number.

We have shown in this study that for every pair of positive integers m and k where m is at least three, there exists a unicyclic graph G with m-cycle accessibility

number exactly equal to k. In addition, for every pair of positive integers m and n with the property that m is at most n and m is at least three, we developed an algorithm in generating a connected graph G of order n with m-cycle accessibility number equal to n-m. We have also characterized graphs which have m-cycle accessibility number equal to zero and those with m-cycle accessibility number equal to one. Lastly, the induced cycle accessibility number of some special graphs and graphs resulting from some binary operations are generated.

Keywords: distance, induced cycle, k-accessible, cycle accessibility, unicyclic

CMPSD-3

INDUCED CYCLE COVERING OF GRAPHS

Frances Mae C. Dumalagan, Euler Yoland B. Guerrero
Gillian Sofia L. Samson*, Thea Lynn P. Coronel
and Rosalio G. Artes, Jr.

Department of Mathematics, College of Science and Mathematics
Mindanao State University - Iligan Institute of Technology
Andres Bonifacio Avenue, Tibanga, 9200 Iligan City
*Email: misyr_gsls@yahoo.com

Let G be a connected graph such that for every vertex v in the vertex set of G, the degree of v in G is at least 2. An induced cycle of G is a cycle in G induced by a subset of $V(G)$. A family $\mathcal{S}=\{S_1,S_2,\ldots,S_k\}$ of subsets of $V(G)$ is an induced cycle cover of G if for every $i=1,2,\ldots,k$, the subgraph induced by S_i is a cycle in G and for every edge e in the edge set of G, there exists r in the set $\{1,2,\ldots,k\}$ such that e in an edge of the graph induced by S_r. The induced cycle covering number of G is given by $icc(G) = \min\{|S|: S \text{ is an induced cycle cover of } G\}$.

We have shown in this paper that for every pair of positive integers n and k where n is at least 4 and $3k$ is at least n, there exists a connected graph G of order n with cycle covering number equal to one more than k. We also established sharp bounds for the induced cycle covering number of a graph. Moreover, we characterized graphs with induced cycle covering number equal to one. In addition, we determined the induced cycle covering number of cycle, fan, wheel, platonic solids, complete graph, complete bipartite graph, and graphs resulting from the join and corona of two non-empty graphs.

Keywords: induced cycle, induced cycle covering number, platonic solids

CMPSD-4

INDUCED PATH ACCESSIBILITY AND DECOMPOSABILITY NUMBERS OF GRAPHS

Dexter J. Resullar, Mary Joy F. Luga*, and Rosalio G. Artes, Jr.

Department of Mathematics, College of Science and Mathematics
Mindanao State University - Iligan Institute of Technology
Andres Bonifacio Avenue, Tibanga, 9200 Iligan City
*misyr_mjfl@yahoo.com

An m-path of a graph G is a path in G of order m induced by a subset of $V(G)$. For a connected graph G, the distance $d_G(u,v)$ between two vertices u and v in G is the length of a shortest path joining u and v in G. We say that G is an m-path k-accessible graph if there exists an m-path P_m of G such that for every vertex v in the vertex set of G, there exists a vertex u in the vertex set of P_m such that $d_G(u,v)$ d" k. The m-path accessibility number of G is given by $g_m(G) = \min\{k: G \text{ is an } m\text{-path } k\text{-accessible graph}\}$.

A subset S of $V(G)$ is an m-path decomposable set if there exists a collection $C = \{S_1, S_2, S_3, \ldots, S_r\}$ of subsets of S such that for each $i = 1, 2, 3, \ldots, r$, the subgraph induced by S_i is an m-path in G, S_i "$S_j = \emptyset$ for i '" j, and the union of the elements of C is the set S. The m-path decomposability number of G is given by $\Gamma_m(G) = \max\{|S|: S \text{ is an } m\text{-path decomposable subset of } V(G)\}$.

In this study, we provided necessary and sufficient conditions for a graph G to have an m-path accessibility number equal to one and those with m-path decomposability number equal to its order. We also established results on the m-path accessibility number and m-path decomposability number of path, cycle, wheel, fan, complete graph, complete bipartite graph, and graphs resulting from the join and corona of two connected graphs. Moreover, we have shown that for every pair of positive integers m and k, there exists a graph G such that $g_m(G) = k$. Further, we have shown that for any pair of positive integers n and m where m d" n and m divides n, there exists a graph G of order n with $\Gamma_m(G) = n$.

Keywords: distance, induced path, k-accessible, accessibility number, decomposable set, decomposability number

CMPSD-5

ON THE SPAN AND EXTENT OF UNIT-DISTANCE GRAPHS IN THE PLANE

Severino V. Gervacio[1], Hiroshi Maehara[2], Joselito A. Uy[3]*

[1]Mathematics Department, De La Salle University, Manila
[2] College of Education, Ryukyu University, Okinawa, Japan
[3]Mathematics Department, MSU-Iligan Institute of Technology, Iligan City
Tel: 0632214050 loc 140; E-mail: jauy@math1.msuiit.edu.ph

A unit-distance graph in the plane is a graph whose vertices can be represented by distinct points in the plane such that the distances between pairs of points representing adjacent vertices are all equal to 1. For each unit-distance representation of a finite unit-distance graph G, there is a smallest circumscribing circle. The infimum of the diameters of these circles, taken over all unit-distance representations of G, is called the span of G. On the other hand, the supremum of the diameters of all such circles is called the extent of G.

It is natural to think that the span and the extent of a unit-distance graph are related to its diameter. We show here that for any given real number $\varepsilon > 0$, there exists a unit-distance graph G in the plane such that the ratio of the span of G to the diameter of G is less than e. Also, we prove that the extent of G does not exceed $2\sqrt{3}/3$ times the graph-theoretic diameter of G. We show further that for every integer $d \geq 1$, there exists a unit-distance graph G in the plane with diameter d and extent equal to $2d\sqrt{3}/3$.

Keywords: unit-distance graph, span, extent, diameter of a graph

CMPSD-6

MISSING TERMS OF RELLICH INEQUALITY

Alnar L Detalla[1], Toshio Horiuchi[2], Hiroshi Ando[2]

[1]Department of Mathematics, Central Mindanao University, Musuan Bukidnon
[2]Department of Mathematical Science, Ibaraki University, Mito City, Japan
Email: al_detalla@yahoo.com

Consider the Rellich inequality

$$\int_{\Omega}|\Delta u(x)|^{p}\,dx \geq \left(\frac{n-2p}{p}\right)^{p}\left(\frac{np-n}{p}\right)^{p}\int_{\Omega}\frac{|u(x)|^{p}}{|x|^{2p}}dx \tag{1}$$

for any $u \in W_0^{2,p}(\Omega)$, where Ω is a bounded domain in $\mathbb{R}^n$ with $0 \in \Omega$, $n \geq 3$, and $1 < p < \frac{n}{2}$. We improve this inequality by adding terms with singular weight of type $\left(\log \frac{R}{|x|}\right)^{-2}$ in the right hand side. We also show that this weight function is optimal in the sense that the inequality fails for any other weight function more singular than this one. As an application, we use the improved inequality in solving weighted eigenvalue problem for the operator

$$L_{\mu}u = \Delta\left(|\Delta u|^{p-2}\Delta u\right) - \frac{\mu}{|x|^{2p}}|u|^{p-2}u$$

Main result

Theorem. *Let $n \geq 3$, $0 \in \Omega$ and Ω is a bounded domain in R^n.*

(1) Noncritical case $\left(1 < p < \frac{n}{2}\right)$

Assume $\gamma \geq 2$, *then there exist* $K = K(n) > 0$ *and* $C = C(n) > 0$ *such that if* $R > K \sup_{\Omega} |x|$

then

$$\int_{\Omega} |\Delta u(x)|^p \geq \left(\frac{n-2p}{p}\right)^p \left(\frac{np-n}{p}\right)^p \int_{\Omega} \frac{|u(x)|^p}{|x|^{2p}} dx + C \int_{\Omega} \frac{|u(x)|^p}{|x|^{2p}} \left(\log \frac{R}{|x|}\right)^{-\gamma} dx$$

(2)

for any $u \in W_0^{2,p}(\Omega)$.

(2) Critical case $\left(p = \frac{n}{2}\right)$

Assume $\gamma \geq \frac{n}{2}$, *then there exist* $K^* = K^*(n) > 0$ *and* $C^* = C^*(n) > 0$ *such that if*

$R > K^* \sup_{\Omega} |x|$ *then*

$$\int_{\Omega} |\Delta u(x)|^{\frac{n}{2}} \geq \left(\frac{n-2}{\sqrt{n}}\right)^n \int_{\Omega} \frac{|u(x)|^{\frac{n}{2}}}{|x|^n} \left(\log \frac{R}{|x|}\right)^{-\gamma} dx + C^* \int_{\Omega} \frac{|u(x)|^{\frac{n}{2}}}{|x|^n} \left(\log \frac{R}{|x|}\right)^{-\gamma-1} dx$$

(3)

for any $u \in W_0^{2,\frac{n}{2}}(\Omega)$.

Keywords: Rellich inequality, Sharp constant, Eigenvalue, p-laplacian.

CMPSD-7

NON-SINGULARITY OF THE COMPLEMENT OF STARPATHS AND COMBS

Helen M. Rara and Mathithias S. Aviles II

Mathematics Department, MSU-Iligan Institute of Technology, Iligan City
Telefax: 063 2214068; Email: helenrara@yahoo.com;
csm-hmr@sulat.msuiit.edu.ph

The adjacency matrix of a graph G having vertices $v_1, v_2, ..., v_n$ is the n x n matrix $A(G)=[a_{ij}]$ where $a_{ij}=1$ if v_i is adjacent to v_j and $a_{ij=0}$ otherwise. We say that a graph is singular if its adjacency matrix is singular, i.e., det $A(G) = 0$; otherwise we say that it is non-singular. Formulas for the determinant of the adjacency matrix of the complement of starpaths and combs are shown in this paper and from these formulas the non-singularity of the complement of these graphs was determined.

The following results are obtained in this study, where $\overline{Cb_n}$ and $\overline{S_nP_m}$ denote the complement of comb and starpath graphs respectively:

1. $$\det A\left(\overline{Cb_n}\right)=\begin{cases}0 & \text{if } n \text{ is odd}\\ (-1)^{n-1}(n-1) & \text{if } n \text{ is even}\end{cases}$$

2. For $n>2$ and $m \geq 1$,

$$\det A\left(\overline{S_nP_m}\right)=\begin{cases}0 & \text{if } m \equiv 0(\text{mod } 3)\\ \left(\frac{m-1}{3}\right)n & \text{if } m \equiv 1(\text{mod } 3)\\ (-1)^{n-1}\left[\frac{n(n-1)(m-2)}{3}\right] & \text{if } m \equiv 2(\text{mod } 3)\end{cases}$$

3. *The comb Cb_n has non-singular complement if and only if n is even.*
4. *The complement of a starpath S_nP_m is non-singular if and only if $m \neq 2$ and m is not divisible by 3.*

Keywords: adjacency matrix, non-singular graph, starpath, comb

CMPSD-8

TRIMMED MEAN AS AN ADAPTIVE ROBUST ESTIMATOR OF A LOCATION PARAMETER FOR WEIBULL DISTRIBUTION

Carolina B.Baguio

MSU-Iligan Institute of Technology, Iligan City
Tel: 090635434077; Email: cbbaguio@yahoo.com

One of the purposes of the robust method of estimation is to reduce the influence of outliers in the data on the estimates. The outliers arise from gross errors or contamination from distributions with long tails. The trimmed mean is a robust estimate. This means that it is not sensitive to violation of distributional assumptions of the data. It is called an adaptive estimate when the trimming proportion is determined from the data rather than being fixed a "priori'.

In this paper , the efficiency and robustness of an adaptive trimmed mean was examined, where the trimming proportion is determined by a ratio of two trimmed means and compare the efficiency with fixing the trimming proportion. The ratio is taken to be a measure of the tail lengths of the Weibull Distribution when the scale parameter is set to ½. This distribution was chosen because of its versatility in approximating an exponential, a normal, or a skewed distribution depending on the parameter values.

It was found that the Ratio of tail lengths of the Weibull distribution increases in magnitudes as the trimming proportion increases. On the other hand, the asymptotic variances decrease as the trimming proportions increase. It was also revealed empirically that the standard error of the adaptive trimmed mean using the ratio of tail lengths is relatively smaller than when the trimming proportions were fixed a 'priori'.

Keywords: adaptive robust estimate, L-estimates, tail length, location parameter, Weibull distribution

CMPSD-9

SOME TREES WITH DIAMETER 5 AND NON-SINGULAR COMPLEMENT

Severino V. Gervacio[1] and Helen M. Rara[2]

[1]Mathematics Department, De La Salle University-Manila
Email: gervacios@dlsu.edu.ph
[2]Mathematics Department, MSU-Iligan Institute of Technology, Iligan City
Email: csm-hmr@sulat.msuiit.edu.ph, helenrara@yahoo.com

The *adjacency matrix of a graph G* having vertices $v_1, v_2, ..., v_n$ is the n x n matrix $A(G)=[a_{ij}]$ where $a_{ij}=1$ if v_i is adjacent to v_j and $a_{ij=0}$ otherwise. We say that a graph is singular if its adjacency matrix is singular, i.e., det *A(G)* = 0; otherwise we say that it is non-singular. We shall consider here trees with diameter 5 having the additional property that every nonpendant vertex has a constant degree Δ. Such a tree will be called a $T_\Delta(5)$-tree. We shall show an infinite class of (5)-trees with non-singular complement.

The following results are obtained in this study:

1. *Let be disjoint complete graphs, where t 1. Form a new graph G by joining each vertex of to a new vertex* x_i, *I = 1, 2,...,t. Let n =* $n_1 + n_2 + ... + n_t + 1$, *the order of G. Then .*
2. *The graph G in result 1 is non-singular if and only if* $n_i = 1$ *for at most one value of i.*
3. *The maximal* (5)*-tree has a non-singular complement if and only if* > 2.

Keywords: adjacency matrix, non-singular graph, complement of a graph, trees of diameter 5

CMPSD-10

A HELLER-TYPE BOUND FOR THE HOMOGENEOUS FREE DISTANCE OF CONVOLUTIONAL CODES OVER GALOIS RINGS

Virgilio Sison

Institute of Mathematical Sciences and Physics
University of the Philippines Los Baños
College 4031, Laguna, Philippines
Tel: (049) 536-2355, Fax: (049) 536-6610
E-mail: vpsison@up.edu.ph

The distance of a code is one of the most important parameters that measure its ability to detect and correct transmission errors in a noisy communication channel. Among codes of a fixed rate, the larger the distance, the better is the code. Let R be the Galois ring $GR(p^r,m)$ of characteristic p^r and cardinality p^{rm}, which is a Galois extension of the integer ring Z_{p^r} by a root of a monic basic irreducible polynomial of degree m over Z_{p^r}. Galois rings have been the subject of much interest in coding theory because they admit a homogeneous distance with isometric properties, a far reaching generalization of the Lee metric on Z_4. Let $R[D]$ be the ring of polynomials over R in the delay operator D. We consider a rate-k/n convolutional code C over R to be an $R[D]$-submodule of $R[D]^n$ which is the rowspan of a $k \times n$ polynomial encoder matrix $G(D)$ with linearly independent rows. A homogeneous weight with average value Γ is applied on R and extended naturally to C. We prove that the homogeneous free distance of C is bounded above in terms of Γ, the encoder memory and the parameters of R. This bound generalizes the well-known Heller bound for the Hamming free distance of binary convolutional codes.

Keywords: Galois rings, convolutional code, free distance, Heller bound, Plotkin bound

CMPSD-11

CONSTRUCTION OF LOW COST PC AND MICROCONTROLLER-BASED LOGIC CIRCUIT ANALYZER

Archieval G. Briones and Alvin Joseph J. Faustino*

Physics Division, Institute of Mathematical Sciences and Physics
University of the Philippines Los Banos, College, Laguna 4031
Tel: 63 49 5361841; Fax: 63 49 5366610; Email: ajjfaustino@uplb.edu.ph

This study aims to construct a low cost logic analyzer that analyzes and displays digital signals and state transitions of medium scale logic circuits. A logic analyzer acquires and stores digital data from a digital circuit and displays it so a user can locate and determine the faults and behaviors of a certain digital system under test. It allows the user to look at more lines in a digital circuit which an ordinary oscilloscope cannot do. One big problem with the commercially available logic analyzers is its high cost. The low end version costs around half a million pesos. An electronic enthusiast or hobbyist cannot afford to have this tool at home. The solution is to provide a low cost version of logic analyzers.

A ZiLOG microcontroller was programmed to enable it to acquire data from the circuit under test and transfer the data to the computer through the serial port. The main user-interface software was created using a Graphical User Interface tool and was able to show sufficient amount of data to view the transitions of the signals of the circuits under test.

The analyzer was calibrated by testing it on different signal frequencies using a function generator. The maximum acquisition frequencies derived on this test were 1.46 MHz, 1.11 MHz, 1.06 MHz, and 876 kHz for the 8, 16, 23, and 28 channels respectively. The computed maximum signal frequencies were 146 kHz, 111.8 kHz, 106.9 kHz, and 86.7 kHz for the 8-channels, 16-channels, 23-channels, and 28 channels timing mode respectively. Also a set of medium speed logic circuits was tested and their logic analysis and graphs were recorded and studied.

Results showed that the logic analyzer timing mode was able to analyze medium scale digital circuits that have typical frequencies of around 500Hz to 100 kHz. Although frequencies above this range would still exhibit recognizable transition patterns, the more acceptable signal frequencies must be 10 times the acquisition frequency in order to get more accurate number of samples.

Keywords: Logic Analyzer, Microcontroller

CMPSD-12

FABRICATION OF PERCHLORIC-DOPED POLYANISIDINE FILM USING POLYVINYLACETATE (PVA) AS BINDER

Francis M. Emralino*, Marvin U. Herrera

Materials Physics Laboratory, Physics Division
Institute of Mathematical Sciences and Physics
University of the Philippines Los Baños, College, Laguna 4031
Tel: 63 49 5361841; Fax: 63 49 5366610; Email: fraulin_06@yahoo.com

The authors were successful in drawing the perchloric acid-doped polyanisidine (PAnis) powder into films using the polyvinyl acetate (PVA) as binder. Polyanisidine is a conducting polymer; they are plastics that exhibit metallic behavior. Perchloric acid ($HClO_4$) was used as dopant since it known to improve the electrical properties of polyanisidine. Polyvinyl acetate is a low-cost binder. The authors want to emphasize that PVA was included to serve as binder and not to improve its electrical properties. It is however expected that the inclusion of PVA would decrease the conductivity of the samples since it has lower conductivity than perchloric-doped polyanisidine. It is desired to draw powder polymer into films to increase the manageability of usage which includes conducting straps and coatings. Polyanisidine was synthesized using oxidative polymerization. The resulting polyanisidine powder was mixed with different ratios of PVA to produce the films. It was shown that it is possible to draw PAnis film from using the following mass ratios (PAnis:PVA):1:1, 1:2, 1:3, 1:4, and 1:5. Two sets of the mixtures were casted into silicon oxide and sensitized film which acted as substrates. The silicon oxide substrates were rigid substrate while the sensitized films were flexible substrate. This paper also aims to determined the conductivity of the film from the current-voltage graph using four-point probe.

Keywords: Polyanisidine, Conducting Polymer

CMPSD-13

POLYMER ENTANGLEMENT WITH A MAGNETIC FLUX

Mark Nolan P. Confesor* [a], Jinky B. Bornales [a], Christopher C. Bernido [b], M.V. Carpio Bernido [b]

[a] Physics Department, MSU – Iligan Institute of Technology, Iligan City 9200, Philippines
[b] Research Center for Theoretical Physics, Central Visayan Insitute Foundation, Jagna, Bohol 6308, Philippines

In this paper we consider the entanglement problem of a polymer interacting with a magnetic flux confined along a second polymer oriented along the z-axis. We take the first polymer to lie on a plane subjected to a potential, $V = q\vec{A}\cdot\vec{r}$, where q is the net charge of the repeating unit of the polymer, and $\vec{A}$ the vector potential due to the magnetic flux Φ confined along the straight polymer. Following the differential equation approach of Wiegel, we then calculate the entanglement probability W_n for the first polymer to wind n times around the straight polymer and obtain the result,

$$W_n = R\sqrt{\frac{4\pi}{Nl^2}}\exp\left(-\frac{1}{Nl^2}\left\{2\pi nR + \frac{Nl^2}{2R}\Phi\right\}^2\right),$$ where N is the number of repeating units, each of length l, and R is the distance of the polymer on the plane from the origin. Our result agrees with the earlier result obtained using white noise functional approach.

Keywords: entanglement, winding probabilities

CMPSD-14

TRANSIENT SURFACE PHOTOVOLTAGE ANALYSIS OF SILICON MOSFET TRANSISTOR

Arvin Tan* and Marvin U. Herrera

Physics Division, Institute of Mathematical Sciences and Physics
University of the Philippines Los Baños, College, Laguna 4031
Tel: 63 49 5361841; Fax: 63 49 5366610; Email: rvintan@yahoo.com

The surface band gap states of silicon in Metal-Oxide-Semiconductor Field Effect Transistor (MOSFET) were determined by the technique of Surface Photovoltage (SPV) Spectroscopy under ambient temperature and pressure. The silicon substrate was illuminated with varying photon wavelengths ranging from 400 nm to 1998 nm to monitor the band bending in Metal-Oxide-Semiconductor (MOS) structure. This was done to find surface states position by which the contact potential difference is proportional to the band bending. Illumination of the sample with varying energies reveal two surface states, one at 0.97 eV and the other at 1.05 eV above valence band maximum. These states appeared to be bulk states appearing in the surface, their energy positions are comparable to the impurity binding site energy. The transient measurements in between the surface states were determined from the SPV versus time plots. This was done by illuminating the sample with single light wavelength in accordance with the surface states energy positions by which both has identical distribution of energies between them. The surface photovoltage transient measurements were used in the calculation of the surface stares parameter.

Keywords: Surface Photovoltage Spectroscopy, Metal-Oxide-Semiconductor

CMPSD-15

THE HARMONIC OSCILLATOR IN A UNIFORM ELECTRIC FIELD: A WHITE NOISE FUNCTIONAL APPROACH

Enrico B. Gravador and Normilah D. Lindao

Physics Department, MSU-Iligan Institute of Technology, Iligan City

The Harmonic Oscillator in a uniform electric field is solved using White Noise Path Integration. Streit and Hida (1983) interpret the Propagator as the expectation value of the Feynman Functional, $K(x_1, x_2; 0, t) = E\{\exp[\, iS(x)/\eta]\}$ Operationally, this is given as the T-transform of the Feynman Functional. By a change of variable, the Lagrangian of Harmonic Oscillator in uniform electric field is transformed into the Lagrangian of Harmonic Oscillator plus a constant term.

To implement a White Noise Functional approach, the path is parametrized as Brownian Fluctuations about the sure path, $x(\tau) = y(\tau) + (\eta/m)^{1/2} B(\tau), \quad 0 < \tau < t.$ $\omega = \dot{B}$ is interpreted as a generalized function on an infinite dimensional space. The collection $\{\dot{B}(\tau); \quad \tau \varepsilon R\}$ of generalized functions forms a continuum coordinate system. The action containing the quadratic term in x can be expanded in Taylor series about the sure path $y(\tau) = 0$. Parametrization of the path leads to

$$K(0, x_2; 0, t) = E_\omega^{\,N} \exp\left[(i+1)/2\langle \omega, \omega\rangle - i/\eta\langle \omega, S''\omega\rangle + \frac{iq^2E^2}{\eta 2m\Omega^2}t\right] \quad \delta^1 B(t) - (m/\eta)^{1/2} x_2 \,|\,\}$$

$$K(0, x_2; 0, t) = \left(\frac{m\Omega}{2\pi i\eta \sin \Omega t}\right)^{1/2} \exp\left(\frac{iq^2E^2}{\eta 2m\Omega^2}t + \frac{im\Omega[x_2 - qE/m\Omega^2]^2}{2\eta \tan \Omega t}\right).$$

Getting the T-transform yields the propagator of Harmonic Oscillator in uniform electric field:

$$\Psi_n = (2^n n!)^{-1/2} \left(\frac{m\Omega}{\pi\eta}\right)^{1/4} H_n(\sqrt{m\Omega/\eta}\,(x_2 - qE/m\Omega^2)) \exp(-m\Omega/2\eta)(x_2 - qE/m\Omega^2)^2 - \frac{q^2E^2}{}$$

wavefunctions are

We realize that the energy spectrum and wavefunctions agree with those found by solving the Schrödinger equation.

Keywords:

CMPSD-16

GEOMORPHOLOGICAL CHARACTERIZATION OF THE NOVEMBER 2004 DEBRIS FLOW AND FLOODING IN INFANTA, QUEZON: UNDERSTANDING HAZARDS AND MANAGING RISKS

Ada Liezl Maria C. Lim, Rene Juna R. Claveria*, Teresita R. Perez

Department of Environmental Science, Ateneo de Manila University
Telefax: 02 4264321; Email: rclaveria@ateneo.edu

The Philippines is one of the countries vulnerable to disasters caused by natural calamities due to its geologic setting and geographic location. Flooding, landslides, earthquakes and volcanic eruptions are most common. Calamities due to natural disasters have seemingly been more frequent world wide. The municipality of Infanta, Quezon experienced debris flow and flooding in November 2004, which resulted in the loss of lives and damage to properties.

Characterization of the debris flows, landslides and flooding in Infanta was done to understand better events leading to the November 2004 disaster. Geomorphologic studies were utilized to appreciate better the mechanisms leading to the disaster. Secondary data from the technical studies conducted in Quezon and Aurora were used.

Infanta is a flood plain of the Agos watershed. Geomorphic changes in the Agos River Delta through time had shaped the Infanta landscape. Precipitation in November 2004 was recorded 2400% higher than the long term average rain fall. This contributed to the increase in pore-water pressured and over saturation of the soil. These led to mass movements and debris flows. Artificial dams were formed in both Kanan and Kaliwa Rivers. The breaching of the dams resulted in the high volume of water flow carrying debris and mud. This inundated Infanta.

There were no historical records available on floods, landslides and debris flows in Infanta and neighboring municipalities. However empirical data indicated similar events had happened before.

A portfolio of risk management options was proposed to prepare the local people to the hazards of floods and debris flows. With a better understanding of the natural processes and consequences, integrated floodplain strategies are to be implemented. Sustainable development, ecology and economy should complement the strategies. These will hopefully help Infanta develop, implement and monitor risk management programs.

Keywords: geomorphology, debris flow, flooding, natural hazard, risk assessment, Infanta, Quezon, Agos River

CMPSD-17

GPS-DERIVED PRECIPITABLE WATER VAPOR AT A TROPICAL LOCATION

Lorenzo de la Fuente[1*], Daniel McNamara SJ[2] and Harold Ritchie[3]

[1]Department of Environmental Science, Ateneo de Manila University
Tel: 63 2 4254321; Email: ldelafuente@ateneo.edu
[2]Manila Observatory, Tel: 63 2 4265921; Email: daniel@observatory.ph
[3]Department of Oceanography, Dalhousie University
Tel: 1 902 4543371; Email: hal.ritchie@ec.gc.ca

Zenith Wet Delay (ZWD) is a nuisance component embedded in Global Positioning System (GPS) measurements from which meteorological water vapor (WV) equivalent may be derived. Station PIMO of the International GPS Service (IGS) has operated since 1998, but multi-annual analysis of these records has not previously been done. In this study hourly averages for ZWD and WV equivalent are compiled for monthly, seasonal, annual and multi-annual periods, which should be comparable to standard meteorological moisture observations. Monthly averages are also compiled for seasonal, annual and multi-annual periods with particular focus on the 1999-2000 La Nina, and should reflect above average moisture levels characteristic of the event. Hourly GPS data are also used to calibrate derived WV equivalents against rain gauge measurements during significant storms such as Typhoons Xangsane and Cimaron in 2006, which may provide useful predictors relevant to storm track and intensity.

Keywords: GPS meteorology, water vapor, remote sensing, La Nina, typhoons

CMPSD-18

EXIGUOLIDE, A NEW MACROLIDE FROM THE MARINE SPONGE *Geodia exigua.*

Mylene M. Uy[a*], Shinji Ohta[b*], Mihoko Yanai[c], Emi Ohta[b], Toshifumi Hirata[d] and Susumu Ikegami[b]

[a]Department of Chemistry, MSU- Iligan Institute of Technology
9200 Iligan City, Philippines
Tel.: (063) 221-4051 loc 123; e-mail: csm-mmu@sulat.msuiit.edu.ph
[b]Nagahama Institute of Bio- science and Technology, 1266 Tamura-cho,
Nagahama, Shiga 526-0829, Japan; E-mail: s_ohta@nagahama-i-bio.ac.jp
[c]Natural Science Center for Basic Research and Development &
[d]Department of Mathematical and Life Sciences, Graduate School of Science,
Hiroshima University, 1-3-1
Kagamiyama, Higashi-Hiroshima
739-8526, Japan

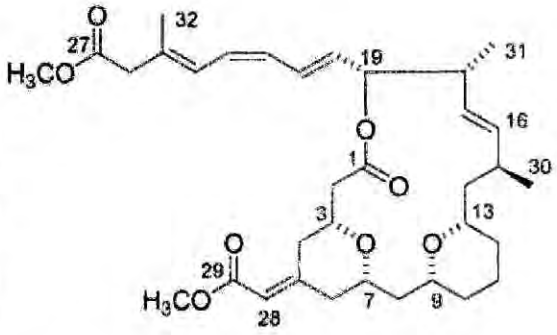

Marine sponges have provided a seemingly inexhaustible supply of bioactive metabolites. In the course of our continuing search for inhibitors on echinoderm fertilization from marine sponges, we isolated a new macrolide designated exiguolide (**1**) from the MeOH extract of the sponge *Geodia exigua* Thiele (order Astrophorida, family Geodiidae).

The gross structure of **1** was determined by interpretation of spectroscopic data. Its relative stereochemistry was elucidated on the basis of NOESY correlations and vicinal ^{1}H couplings. Conformational searches were performed for all possible stereoisomers of **1** using CAChe CONFLEX program with the MM2 force field for energy minimization field (CAChe version 5.5; Fujitsu Co., Tokyo, Japan) to give the only conformational model with 3*R**, 7*S**, 9*R**, 13*S**, 15*S**, 18*R**, 19*R** configuration whose calculated proton distances and dihedral angles were in full agreement with the observed NOE correlations and vicinal ^{1}H couplings. The relative stereochemistry of **1** was supported by the *J*-based configuration analysis method.

Although many biologically active macrolides have been obtained from marine organisms, there are very few compounds having the methoxycarbonylmethylidenetetrahydropyran ring system among them. Exiguolide possesses this unique chemical feature which is also found in the antineoplastic compounds, bryostatins.

Sea urchin (*Hemicentrotus pulcherrimus*) gametes were treated with **1** to investigate its effects on fertilization and egg activation. Concentrations at or higher than 21 μM of **1** prevented fertilization. However, **1** at 100 μM did not affect the development of fertilized eggs up to the gastrula stage.

Keywords: biologically-active compounds; natural products; marine sponges; macrolide; sea urchin

CMPSD-19

BIOTECHNOLOGICAL PRODUCTION OF STRUCTURED LIPIDS: A study on the Triglyceride Species and Fatty Acids of Some Fungal Oils

Laura J. Pham* and Precy M. Rasco

Food, Feeds and Specialty Products Biotechnology Program
BIOTECH, U.P. Los Baños, College, Laguna, 4031
Email: laura@lgn.csi.com,.ph

Structured lipids or tailored fats are being developed now to meet the needs of today's consumer. The enzymatic process of modification is one of the advances in the fats and oils biotechnology which gives an additional level of flexibility in controlling and designing structured lipids or interesterified oils. Our research work in BIOTECH targeted the incorporation of omega-3 fatty acids such as DHA, EPA, α-linolenic acid and omega-6 fatty acid such as γ-linolenic acid and linoleic acid into coconut oil so that a structured lipid containing both medium chain fatty acids providing a dense source of calories which the body can readily use and omega-3 and 6 for important biological functions is prepared through enzymatic interesterification. The current interest in the nutritional role of these fatty acids has stimulated research into their production by a number of fungal sources which are active in the synthesis of polyunsaturated fatty acids.

The present study looked at the oil content and lipid molecular species of oleagineous fungi obtained from the BIOTECH Microbial Culture Collection.Potential oil yielding fungal isolates investigated were originally twenty-four (24) strains but trimmed down to seven (7) strains based on the biomass and

percent oil content. Lipid class analysis of the fungal oils by thin layer chromatography and quantification by the BIOSOFT quantiscan program showed the presence of triglycerides, diglycerides, monoglycerides, free fatty acids, sterols and cholesteryl esters with triglycerides being the major class.

The fatty acid profile of the isolates showed high unsaturation, the highest being that of *Trichosporon inulinum* (BIOTECH strain 2090) at 50.51%. The presence of the omega-6 fatty acid linoleic acid ranged from 0.19 to 18.24% in the fungal oils. Minor polyunsaturated fatty acids detected were γ-linolenic and eicosapentaenoic (EPA) acid.

The triglyceride molecular species were of the USU, SU2 and U3 types (S-saturated; U-unsaturated) which are considered of nutritional importance. Dominant triglyceride molecules are that of PN46 and PN48 and the lowest being PN40.Results of this study showed the promise of fungal oils in the production of structured lipids, the fats of the future.

Keywords: Modification, interesterification, triglyceride, fungal isolates, fatty acids

CMPSD-20

PERFORMANCES AND COLOR EVALUATION OF DYED CROSSLINKED AND UNTREATED COTTON USING ACHUETE (*Bixa orellana*) AND SIBUKAO (*Caealpinia sappam L.)* Dye Powder

Lorna T. Enerva[1], Elbert C. Carillo[2], Maria Christie A. Cardillo[2], Ryan C. Yutoc[2] and Julius L. Leano Jr.[3]

[1]SciTech R and D Center & [2]College of Science
Polytechnic University of the Philippines
[3]Philippine Textile Research Institute, DOST, Bicutan, Taguig Manila
Email: lornaenerva@yahoo.com

Cotton fabric samples were prepared for dyeing. They were desized, scoured and mordanted. The cotton fabric was dyed using achuete and sibukao dye powder under different conditions, dyeing temperature (room temperature and boiling), liquor ratio (1:20, 1:30 and 1:50) and dye concentrations (4%, 6% and 8%). Half of the cotton fabric samples were subjected to crosslinking and the other half remained untreated. The samples were evaluated for colour fastness performances. The dye absorbed by cotton was analyzed using UV-Vis spectroscopy.

The absorption curves under different dyeing conditions revealed that the higher the dye concentration, higher temperature and lower liquor ratio resulted in higher dye absorption of cotton using both achuete and sibukao powder.

The absorption curves also revealed that the rate of dye absorption of achuete on $CuSO_4$- mordanted cotton was rapid during the first 30 minutes and slowed down after 60 minutes while sibukao, alum and $CuSO_4$ mordanted cotton showed relatively rapid dye absorption during the first 30 minutes which it slowed down with minimal absorption further taking place.

The results of the colour fastness dye exhaustion for achuete and sibukao dyed cotton revealed the effectiveness of crosslinker when applied to cotton. It enhanced the resistance of dyed cotton under different dyeing conditions as shown by colour fastness tests to light and washing.

Keywords: mordant, dye, crosslinking, colour fastness, achuete, sibukao

CMPSD-21

SPME—A SIMPLE, SOLVENT-FREE EXTRACTION METHOD FOR FLAVOR COMPOUNDS FROM GLUTEN HYDROLYSATE AND GLUCOSE

Marissa V. Romero

Rice Chemistry and Food Science Division
Philippine Rice Research Institute, Maligaya
Science City of Muñoz, 3119 Nueva Ecija
Telefax: (044) 456-0277; -0258; local 245
Email: mvr@philrice.gov.ph; marissa9396@yahoo.com

Solvent extraction is the conventional method in isolating target compounds from a sample matrix. It is, however, plagued with possible health hazards posed by the organic solvents and environment problem due to waste disposal. In this study, solid phase microextraction (SPME) was evaluated as alternative to solvent extraction in obtaining the volatile compounds from enzymatically hydrolyzed gluten and reducing sugar. SPME is a simple, rapid, and solvent-free extraction technique based on the partitioning equilibrium of analytes between the sample matrix and the extraction medium. It is also compatible with common separation techniques such as gas chromatography and high performance liquid chromatography.

To increase the utilization of gluten, a waste by-product of starch processing, it was hydrolyzed with Umamizyme and Glutaminase to obtain substrates for Maillard reaction. The hydrolysates were heated with glucose at 155°C for two hours. The flavor compounds generated were then isolated by SPME and analyzed by gas chromatography. To optimize the extraction efficiency, various parameters such as SPME fiber, sample pH, and extraction temperature were investigated. Polydimethylsiloxane (PDMS), polydimethylsiloxane-divinylbenzene (PDMS-DVB), and carboxen-polydimethylsiloxane (CAR-PDMS) were evaluated as polymer stationary phase of the SPME fiber. Based on the peak areas, CAR-PDMS exhibited the best extraction performance, suggesting that the isolated analytes were mostly bipolar compounds with relatively low molecular weights. Sample pHs 3.0, 6.0, and 9.0 and extraction temperatures 20 °C, 40 °C, and 60 °C were also studied. The most basic pH and the highest temperature gave the best results, indicating the influence of these parameters in the distribution of an analyte in the different phases and the speed of mass transfer. By optimizing the extraction conditions, SPME was found to be a suitable, simpler, and more environment-friendly extraction method for flavor compounds generated from the Maillard products of hydrolyzed gluten and glucose.

Keywords: solid-phase microextraction, gluten hydrolysate, Umamizyme, Glutaminase, Maillard reaction, polydimethylsiloxane, polydimethylsiloxane-divinylbenzene, carboxen-polydimethylsiloxane

CMPSD-22

FLAVORFUL RICE WINE FROM LABORATORY PREPARED *Bubod* (STARTER CULTURE)

Ma. Jophine C. Ablaza, Amelia M. Valerio, Henry F. Mamucod and Evelyn H. Badonill

Rice Chemistry and Food Science Division, Philippine Rice Research Institute,
Central Experiment Station, Science City of Muñoz
Nueva Ecija, 3119 Philippines
Telefax Number. 044-4560-285/258 local 245
E-mail Address. mjcablaza@philrice.gov.ph

Markets for rice wine become more competitive as rice wine consumption continues to expand. The shelflife of rice wine lies in the quality of *bubod* (starter culture) used for production. The availability of *bubod* manufactured through hygienic and reliable method will therefore provide more income to wine producers.

As such, there is a vital need for the determination of the fermentation efficiency and storage stability of laboratory-prepared (rejuvenated) *bubod* to ensure the production of rice wine with superior and consistent quality in every batch. *Bubod* was rejuvenated fifteen times using commercial mother *bubod* in the first rejuvenation. *Bubod* samples were evaluated for microbial load and efficiency in producing rice wine. Furthermore, the rice wines were assessed for physico-chemical and sensory properties. Despite the large difference in the bacteria ($x10^7$ cfu/g), yeast ($x10^7$ cfu/g) and mold ($x10^5$ cfu/g) count of each of the fifteen rejuvenated *bubod*, the alcohol content (17.95 to 22.15%), pH (3.67 to 3.81), and all sensory properties of the resulting rice wine were comparable to each other. The highest intensity of sweetness, aroma, overall acceptability, total soluble solids and lowest acidity was obtained from the *bubod* rejuvenated for the ninth time. Meanwhile, the yield obtained ranged from 1,095 to 1,350 ml per kg of glutinous rice.

The first rejuvenated *bubod* was also evaluated for its storage stability from 0 to 6 months at refrigerated temperature and rice wine was produced every month. Wine from 3 month old *bubod* had the highest alcohol content and overall acceptability. Bacteria and yeast count decreased as the month of *bubod* storage increased and resulting wine decreased in overall acceptability and sweetness after 3 months.

This study showed that good quality wine can still be obtained even up to fifteen rejuvenations and the first rejuvenated *bubod* can be best stored for 0 to 3 months at refrigerated temperature.

Keywords: *bubod* (starter culture), overall acceptability, physicochemical properties, rice wine, sensory properties

CMPSD-23

ANALYSIS OF DISSIPATION OF TOTAL RESIDUAL OXIDANTS (TRO) AFTER ELECTROCHEMICAL TREATMENT OF SIMULATED SEAWATER

Angelo Carlo Malabanan[1], Catalino Alfafara[1*], Veronica Migo[2], Jovita Movillon[1], and Monet Maguyon[1]

[1] Department of Chemical Engineering, University of the Philippines Los Banos
[2] National Institute of Molecular Biology and Biotechnology (BIOTECH)
University of the Philippines Los Banos, College, Laguna 4031
Telefax: (049)-536-2315 Email: linojp@yahoo.com

Dissipation of total residual oxidants (TRO) after electrochemical treatment of simulated seawater was investigated as an initial step for obtaining operating factors that can be applied to large scale shrimp aquaculture ponds that use electrolysis for ammonia removal. (Excess TRO after electrolytic removal of ammonia are usually dissipated in the field by aeration, to reduce them to levels not harmful to shrimp).

Dissipation experiments at varying aeration levels (after electrolysis) and initial TRO concentrations were conducted. Results show that at the range of aeration rates studied, the TRO decreased with time, coupled with an increase in pH . The rate of dissipation was found to increase initially with increasing aeration rates, but eventually leveled off with time. Mathematical analysis was done on the data to obtain engineering relationships that could be used for scale up and operation in large scale aquaculture ponds.

Keywords: total residual oxidant, air stripping, electrolysis, dissipation, rate constant

CMPSD-24

CHEMICAL COMPOSITION AND RHEOLOGICAL BEHAVIOR OF PASALENG KAOLINITE CLAY DEPOSITS OF PAGUDPUD, ILOCOS NORTE

Dionesio C. Pondoc and Fe B. Pungtilan

Department of Ceramic Engineering College of Engineering
Mariano Marcos State UniversityBatac, 2906 Ilocos Norte
Tel.: +63 77 792 2573 Fax: +63 77 792 2633
Email: dondon_pondoc@yahoo.com

This research study was conducted to determine the chemical composition and to evaluate the rheological behavior of Pasaleng kaolinite clay for its potential utilization in the production of ceramic whitewares. Physical properties such as particle size distribution and chemical composition of the raw clay sample were determined to know the approximate amount of kaolinite clay minerals which governed their rheological behavior. The raw clay samples underwent beneficiation process through sedimentation method.

Three test trials consisted of beneficiated Pasaleng kaolinite clay powder made into fluid suspension (clay slip) with a clay-water ratio of 1:1 and 1:2 and to which was added a deflocculant such as sodium silicate and sodium carbonate. The test clay slips were thoroughly mixed in an electric blender for 2, 3, 5, and 7 minutes. The rheological property like specific gravity was determined using the

specific gravity cup method and viscosity was measured by Zahn-cup method. Methylene blue index (MBI) and cation exchange capacity (CEC) of clay slip were also determined to measure the specific surface area of kaolinite mineral present in the Pasaleng clay deposits.

Results show that the particle size distribution of Pasaleng kaolinite clay consisted of 46.25% retain in 40 mesh, 7.48% retain in 50 mesh, 1.67% retain in 60 mesh, 5.45% retain in 80 mesh, 2.78% retain in 120 mesh, 1.66% retain in 140 mesh, 2.56 retain in 200 mesh and 31.60% passed in 200 mesh. Pasaleng kaolinite clay consisted of 52.58% SiO_2, 26.42% Al_2O_3, 0.53% Fe_2O_3, 0.67% TiO_2, 2.49% MgO, 0.43% CaO, 4.52% Na_2O, 0.94% K_2O and 10.98% loss of ignition. The calculated kaolinite clay mineral was 40.61%. Increased stirring time increased the specific gravity of the slip. The calculated viscosities of the clay slip with and without defloculants increased as the Zahn-cup orifice diameter became larger.

The results of this study revealed that different deflocculants had different effects on clay properties and therefore controlled rheological characteristics.

Keywords: kaolinite clay, chemical composition, and rheological behavior

CMPSD-25

Synthesis of ZN-doped PBTIO via Solid-state Sintering

Jaypee A. Garcia and Marvin U. Herrera*

Physics Division, Institute of Mathematical Sciences and Physics
University of the Philippines, Los Banos, College Laguna
Tel: 63-49-536-1841; Fax: 63-49-536-6610
Email: muherrera@yahoo.com; Japy42_10@yahoo.com

The authors have synthesized Zn-doped PbTiO (PTO) using solid-state sintering method. To be able to produced PTO, stoichiometric amount of PbO, TiO and ZnO were mixed and ground. The mixtures were then pressed into pellet and calcined at 800°C. After calcining, the samples were again ground and pressed into pellet. After which, the samples were sintered at 1,100 °C. Xray- Diffraction (XRD) were used to verify the existence of PTO in the sample. Differential Thermal Analysis (DTA) shows the thermal profile of the samples. Scanning Electron Microscope (SEM) shows the flattening and fusing of grains of sample with 5% Zn mole fraction. The 5% Zn mole fraction also exhibit the lowest melting point among the different concentration prepared.

Keywords: PbTiO, Solid-state sintering

CMPSD-26

MORPHOLOGICAL EVOLUTION OF DIVERSE ZINC OXIDE NANOSTRUCTURES

Ian Harvey J. Arellano*[1,3], Eduardo R. Magdaluyo[2], Denis Aquino[3], Roland V. Sarmago[3] and Leon M. Payawan, Jr[1]

[1] Nanostructures and Surface Chemistry Research Laboratory,
Institute of Chemistry, College of Science
[2] Department of Mining, Metallurgical and Materials Engineering,
College of Engineering
[3] Materials Science and Engineering Program, College of Science
University of the Philippines, Diliman, Quezon City 1101 Philippines
E-mail: iarellano@chem.upd.edu.ph

The morphological evolution of diverse zinc oxide (ZnO) crystal habits was investigated via hydrothermal and carbothermal methods. The mechanism for the hydrothermal growth of ZnO nanowhiskers and its self-assembly to form nanoflowers and nanoblades are presented. ZnO nanoflowers and nanoblades were grown on a copper strip using zinc acetate dihydrate and ethanolamine as precursors at 65°C. Scanning Electron Microscopy (SEM) was employed to deduce the mechanism of growth as a function of substrate's exposure time to the reaction mixture. Flowerlike structures were observed due to clustering at a common seed site to minimize the strain due to lattice mismatch. The shape specificity at higher exposure time is directly attributed to the shape assumed by the nucleation seeds developed at the onset of the reaction. Overexposure of the substrate leads to masking of the ordered nanostructure due to extensive deposition terminating to film formation on the surface. Carbothermal reduction was done on a mixture of ZnO and activated charcoal at varying ratio. Morphological probing using scanning electron microscope (SEM) on the substrate revealed that a specific structure was localized at a certain region on the substrate. This regionalization is due to the difference in the degree of exposure of the substrate to the vapor of the precursor as a result of the vapor current induced by the setup. The presence of a vapor current results to inhomogeneity of the boundary diffusion layer causing the production of various regions in the substrate containing different structures like nanowires, microrods, microtubes and tetrapods. The as-grown nanostructures adapted the hexagonal crystal lattice of ZnO as shown from xray diffraction (XRD) data. The photoluminescence spectra of these structures were taken and a band gap emission at around 390 nm was observed corresponding to a band gap energy of 3.20 eV.

Keywords: zinc oxide, carbothermal reduction, hydrothermal, crystal habit